Femtosecond Four-Wave Mixing Spectroscopy of Molecular Aggregates

ARTICLE *in* THE JOURNAL OF PHYSICAL CHEMISTRY B · SEPTEMBER 1997

Impact Factor: 3.3 · DOI: 10.1021/jp9639713

Femtosecond Four-Wave Mixing Spectroscopy of Molecular Aggregates

E. Gaizauskas[†] and L. Valkunas*[,‡]

Vilnius University, Sauletekio al.10, 2054 Vilnius, Lithuania, and Institute of Physics, Gostauto 12, 2600 Vilnius, Lithuania

Received: December 3, 1996; In Final Form: April 16, 1997[⊗]

Two-photon resonance-enhanced four-wave mixing processes taking place in circular aggregates are considered theoretically with respect to their influences on pump−probe difference absorption measurements. Remarkable changes of the signal spectra around the zero time delay arising from the two-photon resonance transitions to the two-exciton states were discovered. Time- and frequency-resolved pump−probe measurements in the vicinity of zero delay times were shown to be sensitive to the manifestation of two-exciton states and, consequently, may be used for the analysis of the transition dipole orientation of the individual molecules as well as the extent of exciton localization in the circular aggregates.

1. Introduction

New structural data of well-organized circular aggregates of bacteriochlorophyll (Bchl) molecules in peripheral (LH2)[1−3] and core (LH1)[4] photosynthetic bacterial antenna pigment−protein complexes stimulate the assumption of the coherent excitons being responsible for the spectral peculiarities and excitation kinetics in these systems[5−7] (see also Liuolia et al., submitted to *J. Phys. Chem.*, and Novoderezhkin, submitted to *J. Phys. Chem.*). A number of theoretical and experimental studies have been concentrated to different aspects of the pump−probe measurements of coherent excitons in molecular aggregates (see ref 8 for a review). For these systems the pump pulse predominantly creates the population of the single exciton in the lowest k-states. Therefore, one-exciton transitions are bleached after the pump pulse action during the lifetime of the exciton states being measured with a delayed probe pulse. In addition, the excited-state population of the single exciton gives rise to absorption on one- to two-exciton transitions that have been already demonstrated to be present in J-aggregates.[9,10] In this case the absorption is somewhat blue-shifted compared to the bleach, which, in principle, as was demonstrated in recent papers,[11−15] can be applied to determine the exciton coherence length.

Nevertheless, these investigations were mainly concentrated on the quasistationary spectral features, i.e., the evolution of excitations after some kind of equilibration in the system was taken into consideration. In this case the changes of the delayed probe pulse are related to simple changes of absorption or stimulated emission processes, induced in the system by the pump pulse. It is noteworthy that material coherence in this case manifests itself in spectral changes that in addition are also influenced by the system environment in a great extend, i.e., a correct inclusion of the quantum system−environment interaction is of exceptional importance. This problem, unfortunately, is rather complicated because of the structural complexity of the systems under investigation as well as the similarity of the time scales for the energy transfer, nuclear dynamics, and relaxation. For such principal and tremendous difficulties, a general theory describing the manifestation of one- and two-exciton states in transient four-wave spectroscopy by taking all the complexity of system−light as well as system−environment interactions is far from its final formulation and development. Thus, various simplified models of the dynamical system in the presence of the interaction with a bath are usually considered.[6−19]

On the other hand, if the measured signal at negative time delays and/or close to a zero delay time is taken into account with a larger precision (i.e., when the induced polarization in the system is evidently resulted from the interaction of the dynamical system both pump with and probe fields), analysis of the coherent part of the signal may be useful for spectroscopic applications as it displays both light fields and material coherences. From this point of view, the coherent part of the signal may be used by investigating the relaxation of excitations in photosynthetic light harvesting complexes since it may be regarded as displaying material coherence.

This (coherent) part of the signal sometimes is regarded as "coherent artifact" of the pump−probe measurements. Balk and Fleming[20] were the first who showed how the coherent spike can provide the information about the coherence (phase relaxation) of the electronic transition. Until recent years, such kind of investigations was focused on the time dependence of the signal. And only very recently[21] both time- and spectra-resolved measurements corresponding to a special modification of the pump−probe spectroscopy were proposed to be considered for monitoring the upper transition in the three-level system. This measurement, in principle, is also based on the analysis of the coherent part of the signal.

Here we will concentrate on the discussion of time- and spectra-resolved evidence of the coherence in intermolecular interactions in order to distinguish the structural arrangement (orientation of the individual dipoles) of the coherently linked molecular complexes. Specifically, we will provide the theoretical analysis of the pump−probe spectroscopy, developed for one-dimensional exciton systems of circular aggregates and focus on the time-resolved spectra of such kind of aggregates in the vicinity of zero delay time. As a characteristic feature of aggregated systems we note the remarkable changes of the signal spectrum around the zero time delay arising from the two-photon resonance-enhanced four-wave mixing processes, which are due to a presence of the electronic level being close to the two-photon resonance transition. This feature, in principle, may serve for the analysis of the transition dipole orientation of the individual molecules.

[†] Vilnius University.
[‡] Institute of Physics.
* Corresponding author.
[⊗] Abstract published in *Advance ACS Abstracts,* August 15, 1997.

S1089-5647(96)03971-5 CCC: $14.00

2. Energy Spectra of Aggregated States in Circular Chains

In this section we recall a well-known approach[22−26] based on the calculation of the collective excitonic states, which will be used further (in section 3) to simulate the transient absorption spectra as would be obtained in four-wave mixing spectroscopy. Here we follow the pioneering work of Chesnut and Suna,[22] who were the first by analyzing the energy spectrum of the collective excitation in linear aggregates. We consider the spectra of the media consisting of an ensemble of N two-level molecules arranging a periodic chain (circular aggregates having C_N symmetry and molecular transition energy being ϵ_n, where n enumerate molecules in the chain) and being coupled by the nearest-neighbor dipole−dipole interaction. In this, the vector of transition dipole moment $\vec{d}_n$ of the nth molecule makes some angle with the circle plane:

$$\vec{d}_n = d_{||}\vec{x}\cos(\partial n) + d_{||}\vec{y}\sin(\partial n) + d_{\perp}\vec{z} \qquad (1)$$

where $\vec{x}$ and $\vec{y}$ are the unit vectors of the Cartesian coordinates in the plane of the circular aggregate and $\vec{z}$ is the unit vector perpendicular to the plane. Consequently, the dipoles of the individual molecules align in such a way that all dipole−dipole interactions may by considered being equal. The Hamiltonian for this molecular chain may be written as follows:

$$H_0 = \sum_{n=1}^{N}\epsilon_n B_n^+ B_n + J\sum_{n=1}^{N-1}(B_n^+ B_{n+1} + B_{n+1}^+ B_n) \qquad (2)$$

where raising (lowering) operator B_n^+ (B_n) describes the excitation of a molecule at site n and obeys the commutation relations for paulions. In the case of the homogeneous chain ($\epsilon_n = \epsilon$, $n = 1, ..., N$) the following fermionic operators C_n:

$$C_n = \exp(\pi i\sum_{m=1}^{n-1}B_m^+ B_m)B_n \qquad C_n^+ = B_n^+\exp(-\pi i\sum_{m=1}^{n-1}B_m^+ B_m) \qquad (3)$$

can be determined, and the subsequent canonical transformation, defined by $\xi_k^+ = \sum_{n=1}^{N}\phi_{kn}C_n^+$, can be used for diagonalization of Hamiltonian (2) giving[22]

$$H_0 = \sum_{k=1}^{N}\Omega_k\xi_k^+\,\xi_k \qquad (4)$$

Expansion coefficients ϕ_{kn} determines the amplitude of the kth eigenfunction on the site n, and Ω_k is the transition energy to the kth state. After solving the eigenvalue problem by using periodic boundary conditions, the following equations for the corresponding transition frequencies and coefficients are obtained:

$$\phi_{kn} = \sqrt{1/N}\exp(ikn) \qquad \Omega_k = \epsilon + 2J\cos k \qquad (5)$$

where $k = 2\pi j/N$ for the number of the excitations in the chain being *odd* and $k = \pi(2j-1)/N$ for the number of the excitations in the chain being *even*. In general, unlike the case of the open chain, the eigenstates of the cyclic aggregates in the mth energy manifolds cannot be generated by the application of creation operator ξ_κ^+ to the $(m-1)$th energy manifold. Despite that, the diagonalized states of Hamiltonian 4 allows, however, creation of the two-exciton state by generating two "fermions" at the same time.[22] In other words, the eigen functions of M-exciton states ψ_M can be easily written in terms of summation over the appropriate Slater determinants, i.e., for $M = 1$ and 2

$$\psi_1(k) = \sum_{n=1}^{N}\phi_{kn}|n\rangle \qquad (6)$$

$$\psi_2(k_1k_2) = \sum_{n_2>n_1}^{N}\sum_{n_1=1}^{N-1}\{\phi_{k_1n_1}\phi_{k_2n_2} - \phi_{k_2n_1}\phi_{k_1n_2}\}|n_1n_2\rangle \qquad (7)$$

where $|n\rangle$ is the state with site n excited. Further, for convenience, we will use the Dirac's ket- and bra- vectors when describing the states in both the first $|k\rangle$ and second $|k_1,k_2\rangle$ exciton bands and enumerate these states according to their j number (by taking them as follows: $j = 0, \pm1, \pm2, ..., \pm(N-1)$, N and $j_2 < j_1 = 0, \pm1, \pm2, ..., \pm(N-1)$, N).

It is straightforward now to evaluate the spectra resulting from transitions among ground-state, one-exciton, and two-exciton bands. Let us introduce the operator corresponding to the electric dipole moment $\hat{\mu} = \sum_{n=1}^{N}\vec{d}_n(B_n^+ + B_n)$. The explicit expressions for quantities of interest: $\mu_{01}^{(k)} = \langle k|\hat{\mu}|0\rangle$, the electric dipole matrix elements from the ground state $|0\rangle$ to the $|k\rangle$th state in the first manifold, and $\mu_{12}^{(k,q)} = \langle q|\hat{\mu}|k\rangle$, i.e., the electric dipole matrix element from the kth state in the first manifold to the state characterized by excitonic "wavenumbers" $q = (k_1,k_2)$ in the second manifold, may be calculated by using functions 6 and 7 and read as follows:

$$\vec{\mu}_{01}^{(k)} = \sum_{n=1}^{N}\vec{d}_n\phi_{kn}$$

$$\vec{\mu}_{12}^{(k,q)} = \sum_{n1=1}^{N-1}\sum_{n2=n1+1}^{N}(\vec{d}_{n2}\phi_{k,n2} + \vec{d}_{n1}\phi_{k,n1})(\phi_{k1n1}\phi_{k2n2} - \phi_{k1n2}\phi_{k2n1}) \qquad (8)$$

We illustrate both contributions of one- and two-exciton states by presenting the stick spectra of the aggregate as negative (resulting from the transitions to one-exciton states) and positive (resulting from the transitions from one- to two-exciton states) columns in Figure 1a for the N number of molecules in the circular aggregate being 8 and the ratio $r = d_{\perp}/d_{||} = 0.05$. It is well determined that periodic boundary conditions used in calculations respond for the fact that two spectral lines appear at the negative side indicating two allowed transitions into the lowest states corresponding to $j = 0$ and $j = \pm1$ (the 2-fold degenerate state). Let us note in this connection that when the ratio r decreases, the transition to the lowest exciton state ($k = 0$) becomes increasingly forbidden, whereas the next exciton state gains the oscillator strength. This is why the oscillator strength of the transition to the state $k = 0$ is barely seen in Figure 1 for the given ratio. Because of negligible changes of the oscillator strengths of the positive transition bands (see Figure 1a) when changing ratio r (or the number of aggregated molecules N) the mentioned feature is of great relevance to two-photon resonance-enhanced four-wave mixing processes and may be used for monitoring the orientation of the transition dipole moment in the aggregate. In the following discussions we will analyze two-photon resonance-enhanced four-wave mixing in the circular aggregate and confine ourselves by taking four- level system as an appropriate model for the optical transitions in the circular aggregate (see Figure 1b).

3. Transient Spectra of the Circular Aggregates as Obtained by Means of Femtosecond Four-Wave Mixing Spectroscopy

Following our main goal formulated in the Introduction, we start here with the description of the selective modification of

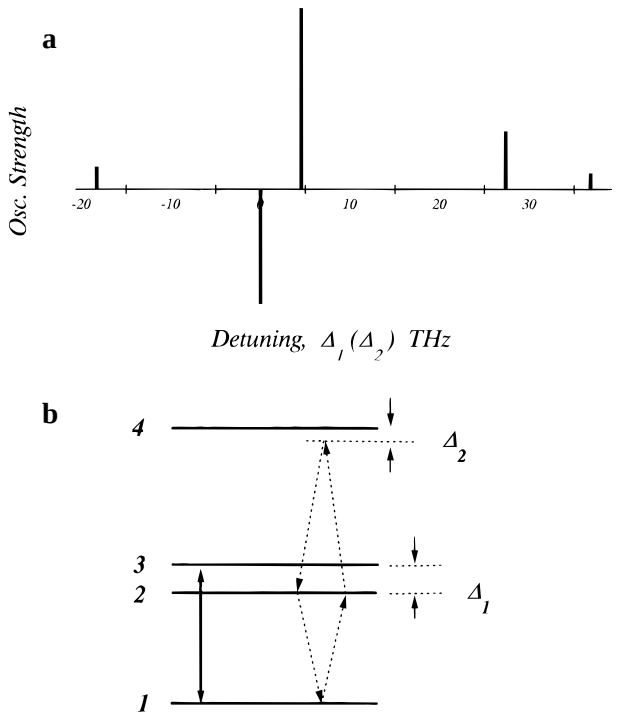

Figure 1. (a) Stick spectra of the circular aggregate ($J = -20$ THz, $N = 8$, $r = 0.1$). Negative bands correspond to the optical transition into the one-exciton manifold, and positive bands define transitions to the two-exciton manifold. The zero-frequency point is taken at one- and two-photon resonance for the negative and positive bands, respectively. (b) Schematic drawing of the four-level quantum system, where 1 is the ground (vacuum) state; 2 and 3 define two dipole-allowed states, correspondingly, i.e., $j = 0$ and $j = \pm 1$ in the one-exciton manifold; while 4 is the two-exciton state being close to the resonance with the applied fields.

pump−probe spectroscopy by describing it as a four-wave mixing process using a reduced number of one- and two-exciton states of circular aggregates. Specifically, we consider the four-level system, in which the ground state is electric-dipole coupled by the external electromagnetic field to the two dipole-allowed quantum states ($j = 0, \pm 1$) in the first excited manifold (see Figure 1b). Further, we take into consideration one of the quantum states (which appears near to the two-photon resonance) in the next manifold and assume electric-dipole allowed transitions to this state from both one-exciton states. For the sake of simplicity, we note the above-mentioned states as follows: 1, the ground state; 2, 3, one-exciton states; 4, the two-exciton state. We are going now to describe absorption changes measured by a weak probe field (having carrying frequency ω and wave vector k_P) in such a medium when exposed to a laser (pump) pulse (having the same carrying frequency ω at slightly different wave vector $\vec{k}_L$). Specifically, we write the electric field as a superposition of the two quasimonochromatic plane-wave pulses:

$$E(t) = {}^1/_2\{E_L(t)\exp(i\vec{k}_L\vec{r} - i\omega t) + E_P(t)\exp(i\vec{k}_P\vec{r} - i\omega t) + cc\} \quad (9)$$

with the (complex) slowly varying electric field envelope functions $E_j(t)$ (j = L, P). The definition *cc* means complex-conjugated terms. Both electric fields are assumed to be linearly polarized in the same direction and the central field frequencies are considered as being in one-photon resonance to the transition $|1\rangle \rightarrow |3\rangle$ and, consequently, appears to be near the two-photon resonance transition to the two-exciton state. The model under consideration can serve as a quite reasonable approach for the description of the four-wave mixing processes taking place in small circular aggregates because due to the resonance conditions only one state in the second excited manifold provides the main contribution to the two-photon resonance-enhanced wave-mixing processes when the central frequencies of light pulses appears near the resonance of the state with the number $j = \pm 1$, i.e., state 3 in our new notation.

Kinetics of the induced absorption changes in the system may be obtained now, in principle, by solving the corresponding equations for the matrix elements of the density matrix, which is defined in the basis of given eigenfunctions as follows:

$$\hat{\rho} = \sum_{i,j}\rho_{ij}|i\rangle\langle j| \quad (10)$$

and governed by the Liuoville equation:

$$i\hbar\frac{\partial\rho}{\partial t} = -[\rho, H_0 + V] + \left\{\frac{\partial\rho}{\partial t}\right\}_{\text{rel}} \quad (11)$$

The Hamiltonian in eq 11 consists of the unperturbed part H_0 and the perturbation V due to the external optical fields applied. The last terms in eq 11 accounts for all complexity of the relaxation. In general, for the aggregates whose size are smaller than an optical wavelength, the total Hamiltonian H in the given basis can be written as follows:

$$H = \begin{bmatrix} \Omega_1 & \mu_{12}E & \mu_{13}E & 0 \\ \mu_{21}E & \Omega_2 & 0 & \mu_{24}E \\ \mu_{31}E & 0 & \Omega_3 & \mu_{34}E \\ 0 & \mu_{42}E & \mu_{43}E & \Omega_4 \end{bmatrix} \quad (12)$$

Here we enumerate the eigenenergies of the system by noting Ω_i (i = 1, 2, 3, 4) and the dipole matrix elements μ_{ij} respond for the transitions $|i\rangle \rightarrow |j\rangle$.

Hamiltonian 12 does not contain the electric dipole transition to the two-exciton states. Nevertheless, the unitary transformation which changes the initial states to the new ones may be found by making use of the small parameter $\lambda \propto \mu_{ij}E/(\Omega_i - \Omega_j - h\omega)$ for the $1 \leftrightarrow 2$ and $2 \leftrightarrow 4$ transitions, correspondingly, and after that the problem can be reformulated and solved in terms of new (transformed) density matrix $\tilde{\rho}$.[27−31] For the light field being in resonance to the transition $|1\rangle \leftrightarrow |3\rangle$, the denominator of this parameter contains nothing but the energy offset between states 1 and 2, which can easily be found from eq 5 and reads as $2J[1 - \cos(2\pi/N)]$. Thus, for typical values of $J \approx -10THz$ and the pump pulse duration 0.1 ps, this perturbative four-level approach (see Figure 1) is fulfilled for N being not too large. Therefore, we will assume $N = 8$, which resembles the symmetry of the LH2 in *Rs. molishianum*.[3] In this new representation and by means of the usual rotating wave approximation the modified optical Bloch equations for the density matrix elements describing the excitations in the system read as follows:

$$\frac{\partial\rho_{13}}{\partial t} = i\Delta_1\rho_{13} + i\Lambda^* n_{31} - is\Lambda\rho_{14} - \frac{\rho_{13}}{T_2}$$

$$\frac{\partial\rho_{34}}{\partial T} = i\Delta_2\rho_{34} + is\Lambda^* n_{43} + i\Lambda\rho_{14} - \frac{\rho_{34}}{T_2}$$

$$\frac{\partial n_{31}}{\partial t} = 2i[\Lambda\rho_{13} - \Lambda^*\rho_{31}] - is[\Lambda^*\rho_{34} - \Lambda^*\rho_{43}] - 2W_{31}\rho_{33} + 2W_{43}\rho_{44}$$

$$\frac{\partial \rho_{14}}{\partial t} = i(\Delta_1 + \Delta_2)\rho_{14} - i\frac{2\tilde{\mu}}{\mu_{13}^2}\Lambda^2\rho_{11} - is(\Lambda^*\rho_{13} - \Lambda^*\rho_{34}) - \frac{\rho_{14}}{T_{22}} \quad (13)$$

where

$$\Lambda = \frac{\mu_{13}}{2\hbar}E(t) \qquad n_{ij} = \rho_{ii} - \rho_{ij} \qquad \Delta_1 = \frac{\Omega_3 - \Omega_1}{\hbar} - \omega \qquad \Delta_2 = \frac{\Omega_4 - \Omega_3}{\hbar} - \omega$$

$$\tilde{\mu} = \mu_{12}\mu_{24}/2\left(\frac{\Omega_2 - \Omega_1}{\hbar} - \omega\right) \qquad \bar{\bar{S}} = \mu_{34}/\mu_{13}$$

and the quadrupole matrix element $\tilde{\mu}$ describes a transition to the two-exciton state in the second excited band. Additionally, the terms describing relaxation processes with characteristic constants W_{ij}, T_2, and T_{22} were added to eq 13 phenomenologically. For the sake of simplicity, the terms describing Stark shifts of the perturbed states have been omitted in eq 13. Note that only single-photon processes are taken into account by determining the temporal evolution of the difference of the excitation population n_{ij}.

In the case of the selective pump−probe spectroscopy, which measures the difference transmission (or absorption) spectrum in the probe beam, the appropriate signal $\Delta A(\tau,\omega)$ at a given frequency ω and delay τ between the pump and probe pulses can be defined as follows:

$$\Delta A(\omega,\tau) \sim \mathrm{Im}\{\tilde{E}_\mathrm{p}(\tau,\omega)\, P^*(\tau,\omega)\} \quad (14)$$

where $P(\tau,\omega)$ and $E_P(\tau,\omega)$ are Fourier transforms of the induced polarization and the probe field. In terms of the new (transformed) density matrix elements the equation for the induced polarization reads

$$P(t) = \mu_{13}\rho_{13} + \mu_{34}\rho_{34} + 2E\mu_{12}\mu_{24}\left(\frac{\rho_{14}}{\hbar\omega - \Omega_2 + \Omega_1)} - \frac{\rho_{41}}{\hbar\omega - \Omega_4 + \Omega_2)}\right) \quad (15)$$

The first terms in eq. 15 accounts for the one-photon resonant polarization, whereas the last sum describes the additional contribution to the polarization induced by transitions to the two-exciton states.

Some additional comment on the two-photon resonant four-wave mixing should be stressed at the end of this section. First, only that part of the polarization (as well as population differences), which produces a periodic grating with the wave vector $\vec{K} = k_L - \vec{k}_P$ will contribute significantly to the difference absorption signal due to the phase-matching condition requirements for the four-wave mixing.

To account for such periodicity induced in the media the following expansions were used:

$$n_{31} = \sum_m n_{31}^{(m)} \exp(-im\vec{K}\vec{r}) \quad (16)$$

while

$$\rho_{13} = \rho_{13}{}^{(L)} \exp(-i\vec{k}_L\vec{r}) + \rho_{13}{}^{(P)} \exp(-i\vec{k}_P\vec{r})$$

$$\rho_{34} = \rho_{34}^{(L)} \exp(-i\vec{k}_L\vec{r}) + \rho_{34}^{(P)} \exp(-i\vec{k}_P\vec{r}) \quad (17)$$

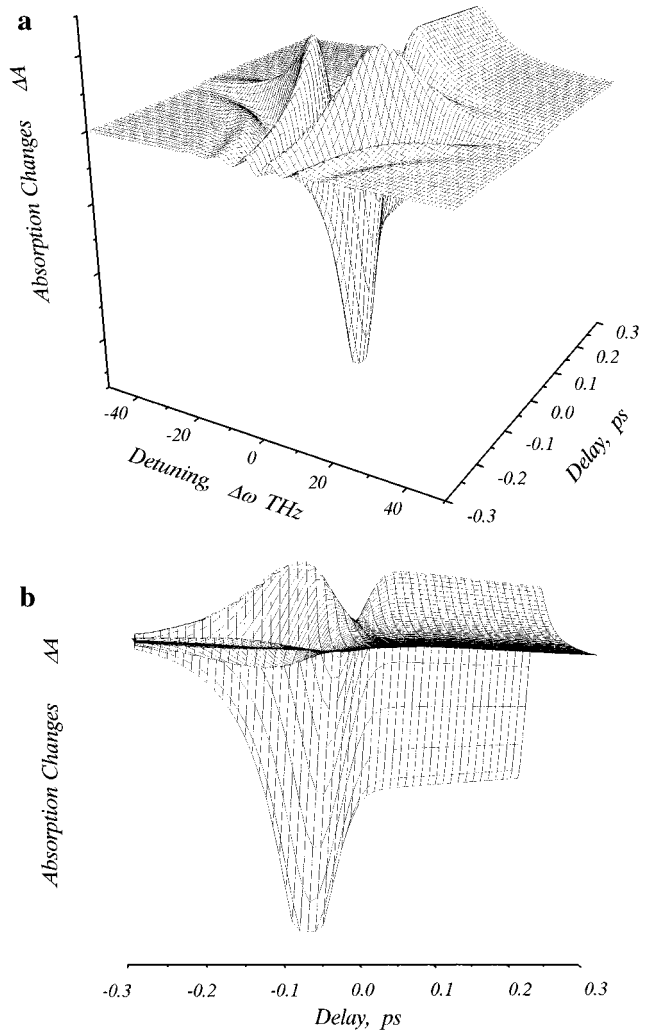

Figure 2. Time- and frequency-resolved absorbance changes for the circular aggregate ($N = 8$, $J = -20THz$) with close to "in-plane" orientations ($r = 0.1$) of the individual dipoles. The three-dimensional plot (a) is supplemented by the projection to the plane [ΔA, delay] (b).

Now, after substitution of the expansions 16 and 17 as well as the complex field 9 into eqs 13, one can separate the time evolution of the induced polarization in the pump and probe directions. We assume that the sample is sufficiently thin, so that scattering orders higher than the first one can be neglected (this reduces the m values to −1, 0, and 1).

4. Discussions

In what follows we present numerical results of time- and frequency resolved spectra as obtained by solving eqs 13−15. In our calculations we have taken both pulses to be Gaussian in shape with the durations 0.09 and 0.01 ps at half-maximum (fwhm) of the intensity for pump and probe pulses, respectively. The corresponding phase relaxation times were taken as follows: $T_2 = 0.06$ ps, $T_{22} = 0.03$ ps. To determine the excitation level, the excitation parameter $\theta_{\mathrm{L,P}} = \int_{-\infty}^{\infty} \Lambda_{\mathrm{L,P}}(t)\, \mathrm{d}t$, i.e., the "area" of the pump (probe) pulse, can be introduced. For calculations these values have been taken as follows: $\theta_\mathrm{L} << 1$, $\theta_\mathrm{P}/\theta_\mathrm{L} = 0.04$.

Evidently, in the case when individual transition dipoles of the molecules in the aggregate are oriented close to "in the xy plane" (i.e., $d_\perp/d_{||} << 1$), the coherent part of the signal (at negative delay times) does not differ much from that characteristic for two-level systems because an optical transition from

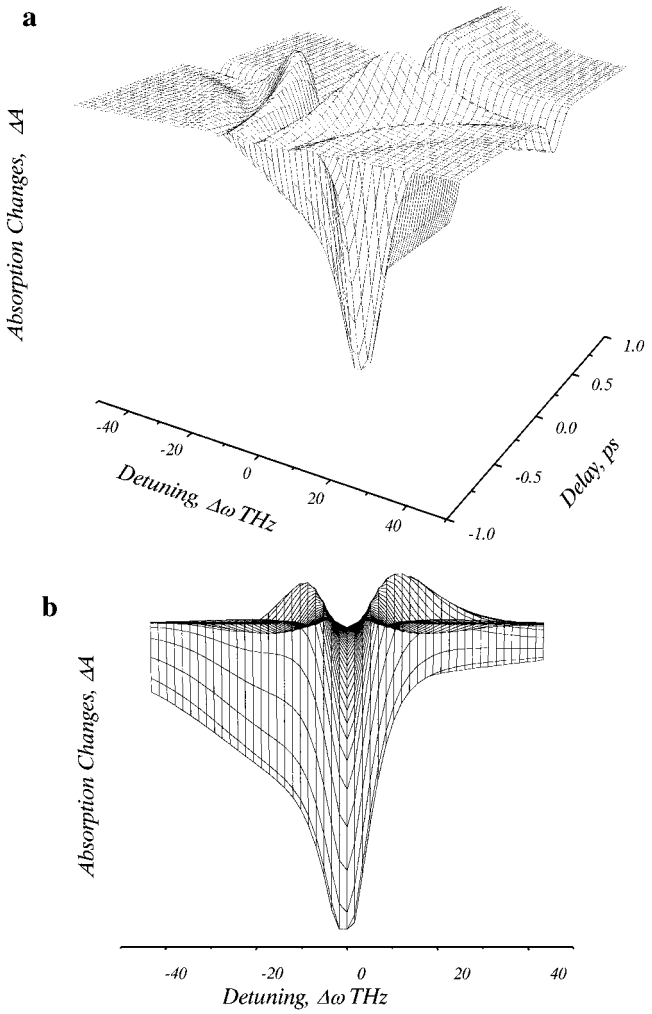

Figure 3. Time- and frequency-resolved absorbance changes for the circular aggregate ($N = 8$, $J = -20THz$, $r = 0.5$). The three-dimensional plot (a) is supplemented by the projection to the plane [ΔA, frequency] (b).

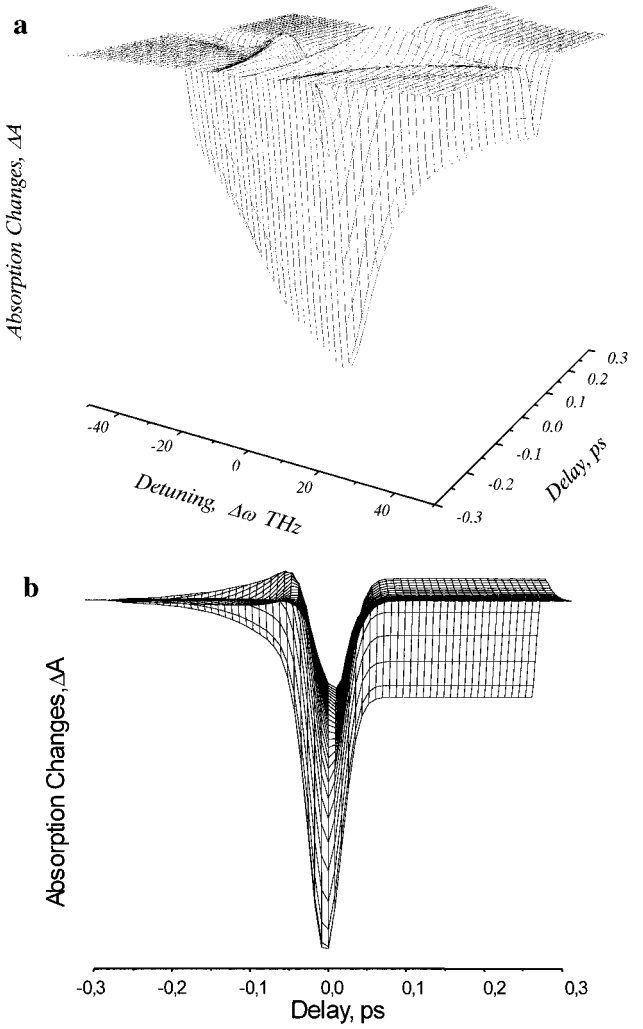

Figure 4. Time- and frequency-resolved absorbance changes for the circular aggregate ($N = 8$, $J = -20THz$, $r = 1$). The three-dimensional plot (a) is supplemented by the projection to the plane [ΔA, delay] (b).

the ground state is allowed into one collectivised state ($|j = \pm 1\rangle$) only. Time- and frequency-resolved absorption changes for this situation in the cyclic aggregate ($N = 8$) is presented in Figure 2. Here the three-dimensional plot of the differential absorption (Figure 2a) is supplemented by a projection (Figure 2b) for the visibility. Coherent oscillations (well-known as a perturbed free-induction decay) in difference absorption spectra appears here for negative delay time, whereas absorption shift ("butterfly" in the difference absorption spectra) due to the transition to the two-exciton state are characteristic for positive delay times. Some asymmetry of the coherent part of the signal, arising as a result of the two-photon-induced polarization on the lower and upper transitions in a three-level system, is not distinguished in this picture (Figure 2) and requires special investigations[21] for the detection of the transitions to the two-exciton state. On the other hand, if we now consider the different situation when individual transition dipoles of molecules in the aggregate are not oriented in the *xy* plane (i.e., $d_\perp/d_\parallel \neq 0$), the two-photon resonance-enhanced four-wave mixing processes becomes increasingly important. As seen from Figure 3 (here for the calculations the same parameters as previously, except the ratio $d_\perp/d_\parallel = 0.5$ is used) the coherent part of the signal at negative delay times has more pronounced asymmetry, especially in the vicinity of the time delay zero, were the pulses overlap. This asymmetry results from the two-photon resonance-enhanced four-wave mixing process which is clearly demonstrated in Figure 4, where the some "artificial" model of cyclic aggregate with the dipoles oriented angle 45° to the *xy* plane was taken, making $d_\perp/d_\parallel = 1$.

Now, taking into account the demonstrated dependence of the transient difference absorption spectra on the two-photon resonance-enhanced four-wave mixing processes, the conclusion about the orientation of the individual dipoles may be obtained when analyzing experimentally femtosecond time- and frequency resolved spectra. To the best of our knowledge, such experiments seems to be quite realistic and may in principle be provided in the nearest future.

Acknowledgment. This research was supported by ISF−Lithuanian Government Joint Grant LH6100.

References and Notes

(1) McDermott, G.; Prince, S. M.; Freer, A. A.; Hawthornthwaite-Lawless, A. M.; Papiz, M. Z.; Cogdell, R. J.; Isaacs, N. W. *Nature* **1995**, *374*, 517.

(2) Freer, A.; Prince, S.; Sauer, K.; Papiz, M.; Hawthornthwaite-Lawless, A.; MacDermott, G.; Cogdell, R. J.; Isaacs, N. *Structure* **1996,** *4*, 449.

(3) Kroepke, J.; Xiche, H.; Muenke, C.; Schulten, K.; Michel, H. *Structure* **1996,** *4*, 581.

(4) Karrash, S.; Bullough, P. A.; Ghosh, R. *EMBO J.* **1995,** *14*−*4*, 631.

(5) Novoderezhkin, V. I.; Razjivin, A. P. *Biophys. J.* **1995,** *68*, 1089.

(6) Sturgis, J. N.; Robert, B. *Photochem. Photobiol.* **1996**, *50*, 5.

(7) Jimenez, R.; Dikshit, S.N.; Bradforth, S. E.; Fleming, G. R. *J. Phys. Chem.* **1996**, *100*, 6825.

(8) Mukamel S. *Principles of Nonlinear Optical Spectroscopy*: Oxford University Press: New York, 1995.

(9) Fidder, H.; Knoester, J.; Wiersma, D. A. *J. Phys. Chem*. **1991**, *95*, 7880.

(10) Minoshima, K.; Taiji, M.; Miasma, K.; Kobayashi, T. *Chem. Phys. Lett*. **1994,** *218*, 67.

(11) Johnson, A. E.; Kumazaki, S.; Yoshihara, K. *Chem. Phys. Lett*. **1993,** *211*, 511.

(12) Novoderezhkin, V. I.; Razjivin, A. P. *Photochem. Photobiol.* **1995,** *62*, 1035.

(13) Pullerits, T.; Chachisvilis, M.; Sundstrom, V. In: *Photosynthesis: from Light to Biosphere*; Mathis, P., Ed.; Kluwer Academic Publishers: Dortrecht, 1995; Vol. 1, p 107.

(14) Bourgel, M.; Wiersma, D. A.; Duppen, K. K. *J. Chem. Phys*. **1995,** *102*, 20.

(15) Chachisvilis, M.; Pullerits, T.; Westerhuis, W.; Hunter, N. C.; Sundstrom, V. *J. Phys. Chem.*, submitted.

(16) Kuhn, O.; May, V.; Schreiber, M. *J. Chem. Phys*. **1994**, *101*, 10404.

(17) Kuhn, O.; Renger, T.; May, V. *Chem. Phys.* **1996,** *204*, 99.

(18) Warns, Ch.; Barvik, I.; Reineker, P.; Neidlinger, T. *Chem. Phys*. **1995**, *194*, 117.

(19) Boeij, W. P.; Pshenichnikov, M. S.; Wiersma, D. A. *J. Phys. Chem*. **1996**, *100*, 11806.

(20) Balk, M. W.; Fleming G. R. *J. Chem. Phys*. **1985,** *83*, 4300.

(21) Gaizauskas, E.; Feller, K.-H.; Valkunas, L. *Opt. Quantum Electron*. **1996,** *28*, 1203.

(22) Chesnut, D. B.; Suna, A. *J. Chem. Phys*. **1963**, *39*, 146.

(23) Juzeliunas, G. *Z. Phys*. **1988,** *D8*, 379.

(24) Spano, F. C.; Mukamel, S. *J. Chem. Phys*. **1991,** *95*, 7526.

(25) Fidder, H.; Knoester, J.; Wiersma, D. A. *J. Chem. Phys*. **1991**, *95*, 7880.

(26) Spano, F. C.; *Chem. Phys. Lett*. **1995**, *234*, 29.

(27) Poluektov, I. A.; Popov, Yu. M.; Roitberg, V. S. *Sov. Phys. JETP Lett*. **1974,** *20*, 533.

(28) Takatsuji, M. *Phys. Rev*. **1975**, *A11*, 619.

(29) Grischkowsky, D.; Loy, M. M. T.; Liao, P. F. *Phys. Rev*. **1975**, *A12*, 2514.

(30) Gaizauskas, E.; Gedvilas G. *Opt. Commun*. **1992**, *91*, 312.

(31) Gaizauskas, E.; Feller, K.-H. *J. Phys. Chem*., submitted.